The Effect of the Aneurysms Diameter on the Mechanical Stress Using Fluid Structure Interaction

Badreddin Giuma s. k [1] , Ali A. Shommaki [2] and Khaled A. Jegandi [3]
E-mail: bbaadre@gmail.com[1]

[1,2,3] The Higher Technical Center for Training and Production- Libya

Abstract

The maximum diameter criterion currently has been widely used to predict the risk of rupture of abdominal aortic aneurysm (AAA). The effect of the aneurysm diameter on the flow pattern and stress distribution is carried out in this study by using the fully coupling fluid structure interaction analysis with hyperelastic material and Non Newtonian fluid models. The results show that the aneurysm diameter effects the direction of flow and also causing increase in the size of vortices as the diameter increased. The stress on the inner wall is higher than the outer wall, and the different between them decreased as the diameter increase. Linear correlation was observed between the aneurysm diameter and maximum stress (R^2= 0.9418). These results have confirmed the aneurysm diameter as an important parameter to predict the aneurysm rupture.

Keywords: *Abdominal Aortic Aneurysm; Fluid Structure Interaction; Geometry Effect; Wall stress.*

1. Introduction

Abdominal aortic aneurysm is a bulge in the wall of the abdominal aorta, affecting 5–7% of people over 60 years[1, 2]. It has the chance of rupture if not surgically treated, where is responsible for 1-3 % of deaths in men from the age 65-85 in developed countries[3]. Currently the surgery is performed only when the risk of rupture is high, where is widely based on the maximum diameter criterion and expansion rate [4-6]. However there are some cases of small aneurysm (<5 cm) ruptured [5, 7-9], and certain of those considered large remain asymptomatic (>5cm) [5, 9, 10].

From biomechanics view point, failure of an AAA wall occurs when the mechanical stress acting on it exceeds its strength. That is considered as an additional indicator to predict the failure of an AAA wall [15-17]. There is no direct technique available to measure the stress in AAA patients[5, 18]. So, several studies [16, 19-26] have used the FEM to computed the wall stress distribution in the wall of AAA, and they have reported it as an efficient tool to predict the aneurysm rupture. In recent years the fluid structure interaction is increasingly being used to calculate the stress in the

wall of aneurysm to obtain the effect of the interaction between hemodynamic and wall deformation in AAA. Some researchers have compared between the FSI, and computational solid stress (CSS), and they conclude the maximum wall stress obtain with FSI is a more accurate than that with CSS[27-30]. Several studies have studied the effect of geometric properties on the distribution of the wall stress in AAAs by using FEM [22, 23, 31-36], and suggested them as important parameters in predict wall stress in the wall of aneurysm.

There are two of reported publications studied the effect of some of geometric properties on the wall stress distribution using FSI [37, 38]. The first studied the effect of asymmetry and wall thickness , whilst the second compared the degree of asymmetry, neck angle and bifurcation angle. Their results showed that these geometry parameters play an important role in wall stress distribution and suggest them as important parameters in computational prediction.
In this study, 3D f-FSI analysis is used to investigated the effect of the aneurysm diameter in the distribution and magnitude of the velocity and the maximum wall stress.

2. Methods

The parameterized geometric model is used to identify the effect of aneurysm diameter, where generated by the MATLAB code and commercial software (SolidWork) in which the cross section at any axial position is circular.
The shape of the aneurysm is defined by a cosine function as given by Eq. (1).

$$r(z) = r_{max} + (r_{max} - r_p)\cos(2\pi L^{-0.999}) \qquad (1)$$

Where r_{max} is the maximum radius of the aneurysm, r_p is the Proximal neck radius, L is the aneurysm region length.
The geometric dimensions of the aneurysm were chosen to be within the range found in clinical observation[13, 39]. The thickness of the wall was assumed to be uniform throughout of model and set to 0.15 cm. The proximal neck was assumed to be a straight tube of diameter 2 cm and length 6 cm. The length of the proximal neck was made longer to allow the flow to be fully developed before entering the aneurysm sack.
The governing equations for blood flow domain and solid domain have been discussed in many of previous publications [27, 29, 30, 37, 40]. However, in this study we have assumed the blood as laminar, homogenous, incompressible, isothermal and Non-Newtonian (Carreau Yasuda model), with transient boundary condition shown in Fig.1 [37]. The fully developed velocity profile was applied at the proximal neck entrance, and the time dependent normal traction was applied normal to the end of iliac bifurcation artery. The hyperelastic material was used to model the aneurysm wall, with fixed

rotation and translation on the inlet and outlet. The boundary conditions that applied to FSI interface was kinematic condition, dynamic condition and no slip condition. Table 1 lists the fluid and structure parameter values used in this simulations.
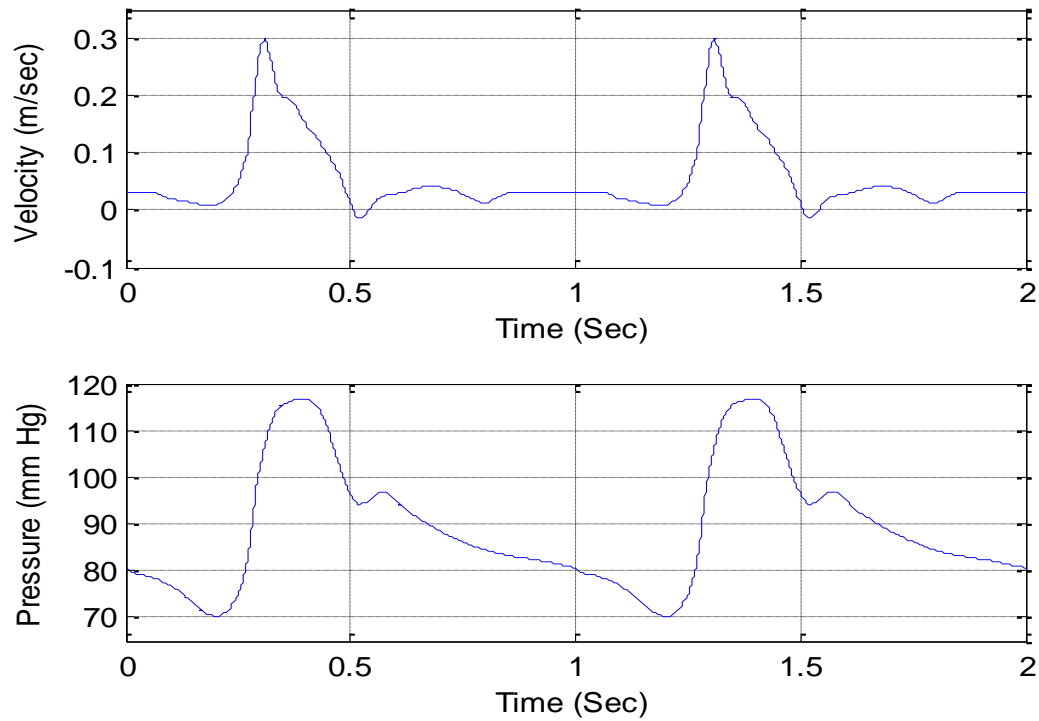

Figure. 1. Transient behavior of the boundary condition.

Table 1. Summary of simulation parameters.

Blood parameters		
Carreau Yasuda Model	$\frac{\eta(\dot{\gamma})-\eta_\infty}{\eta_0-\eta_\infty} = (1 + (\lambda\dot{\gamma})^a)^{(n-1)/a}$ where $\eta_0 = 0.056 Pas,$ $\eta_\infty = 0.00345 Pas$ $\lambda = 1.902s, n = 0.22, a = 1.25$	
Density	$\rho_f = 1050 \ kg/m^3$	
Wall parameters		
Hyperelastic material model	${}_0^t w = c_1({}_0^t I_1 - 3) + C_3({}_0^t I_1 - 3)^2$ Where $c_1 = 0.174 MPa$ $,c_3 = 1.881 MPa$	

Bulk modulus	$K = \dfrac{E}{3*(1-2\upsilon)}$
Young's Modulus	$E = 2.7 MPa$
Poisson's ratio	$\upsilon = 0,45$
Density	$\rho_s = 2000\ kg/m^3$

The fluid equations and the solid equations are formed in their weak form, where the solution procedure of the fluid domain is based on a Petrov- Galerkin formulation [41]. The velocity was interpolated using non-linear functions, and linear or bilinear functions to interpolate the pressure, and coordinates. The mixed interpolation hexahedral elements were used in the solid domain, in which the pressure interpolated by constant functions while the displacement by using bilinear functions. Then both of equations are combine and treated in one matrix and solved by using Newton Raphson method. Two periodic cycles with time step size of 0.001s with relative tolerance of the degrees of freedom less than 10^{-9} in fluid domain, and 10^{-5} contact force tolerance, 10^{-17} displacement tolerance in the solid domain were employed to achieve convergence. In order to achieve the quality of mesh applied in this simulations a sensitivity analysis was conducted for the solid and fluid model separately by using CSM in the solid model and CFD in the fluid model which have been previously used [27, 37, 40, 42,54,55]. The final mesh sizes that selected in this study to balance the CPU simulation times with mesh sensitivity was 0.005mm, where was adopted for all the cases. In addition to the numerical accuracy checks, the present simulation was compared with previous numerical results [28, 29, 37, 38, 40], and a good agreement were obtained.

3. Results and Discussion

Figure 2 shows the velocity vectors within four models with difference diameter at different stage of the second cardiac cycle. The difference between the time stages are observed by the structure of flow pattern where at $D_{an}=3$ cm the streamline of the flow in bulge are smooth during $1.1s < t \geq 1.2s$, before reverse direction at t=1.3s, which causes small recirculation near proximal neck. During $1.4s < t \geq 1.6s$ the blood flow recovers its original direction with disappear the vortices. At t=1.7s the flow direction is reversed again which causes three vortices near the proximal neck. At 1.8s the size of vortices decreases and move near the proximal neck, where are disappeared at 1.9s. In model with diameter ($D_{an}=4$ cm) the vortices start to appears early in the medal of the bulge at t=1.1s, and move to near proximal neck as the blood flow accelerate to t=1.3s, where the

flow direction is reversed. At 1.4s the blood flow recovers its original direction with smooth streamline. At 1.6s the blood flow direction is reversed again causing three vortices near the proximal neck, which disappear at 1.8s. As the diameter increase to 9 cm, and 10 cm, the size of vortices increase and they appear in all of time stage that may cause damaged the blood cells and occurred the platelet activating in the region [2]. The flow pattern in this simulation was significant differences with previously simulation with assumption of rigid wall[39, 43, 44] this because of the viscoelastic dissipation of the flexible wall where the kinetic energy was absorbed during acceleration of the flow in the potential energy to dilate the wall while the stored energy was restored during deceleration of flow. Otherwise this streamlined profile is very similar to that shown in previously FSI analysis[40]. From Fig. 2 we can found that the increase in the diameter of aneurysm effect the direction of flow and also causing increase in the size of vortices, which causing increase in the time for the blood particle to exit the aneurysm, and enlarge the volume of Intraluminal thrombus in the bulge, which have been shown to reduce the wall strength[45-47].
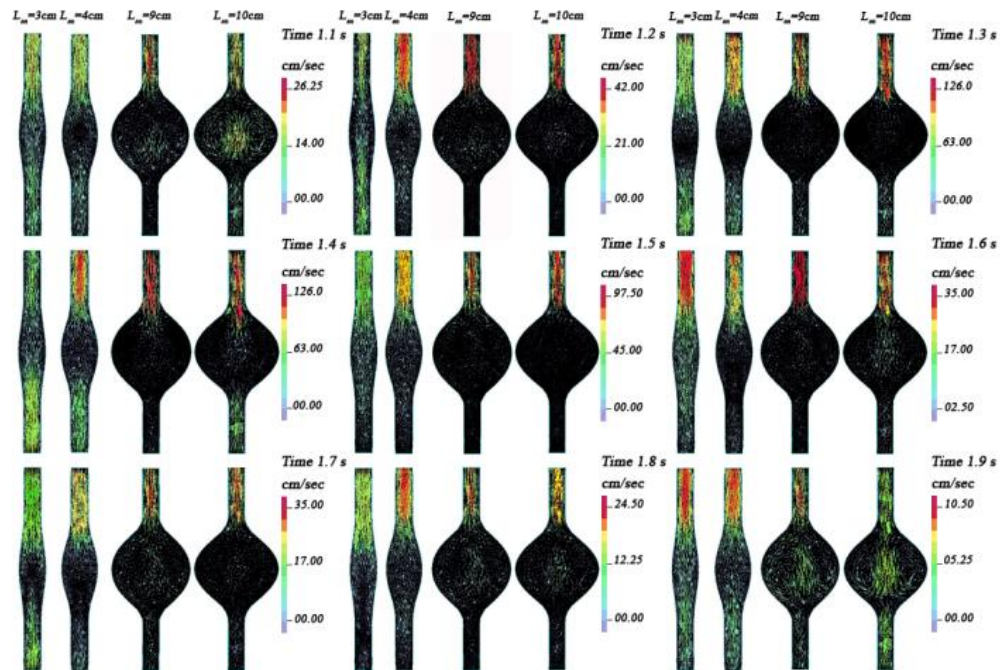

Figure. 2.. The velocity vectors at different stage of the second cardiac cycle through the deferent aneurysm diameter (3, 4, 9, and 10cm)

The distributions of the Von Mises stress of the aneurysm walls induced by transient of blood flow in AAA for model $D_{an}=6$ cm at different periods in the second cardiac cycle are shown in Fig. 3. The Von Mises stress patterns is similar for all the time period, and is located asymmetrical with respect to a centerline, and it increase around the bulge combined, where the highest Von Mises stress occur at peak systolic pressure condition (1.4 s) and located in the bulge near to the proximal and distal end, which agree with previously findings results using FSI [40] and significant different with the solid stress simulation (CSS) [27, 28, 40]. This because they ignore the effect of

the hemodynamic. A previous comparison between the FSI and CSS analysis have also reported this difference. For example the stress distribution found by Borghi et al [48] was higher than that reported by Leung et al[30] and this because the internal pressure apply in the first study was lower than the second one so the pressure drop along the aneurysm was higher. Scotti et al [40] have reported it higher than that found by Borghi et al [48] and this because of the wall thickness in the first result was 50% less than the second one, hence the thinner wall is more sensitive to the internal pressure, Papaharilon et al[49] have used decoupled structure and fluid approach and have shown it higher than that found by Borghi et al [48]. However in all these results the distribution stress in the CSS solution is underestimated in comparison with FSI solution.
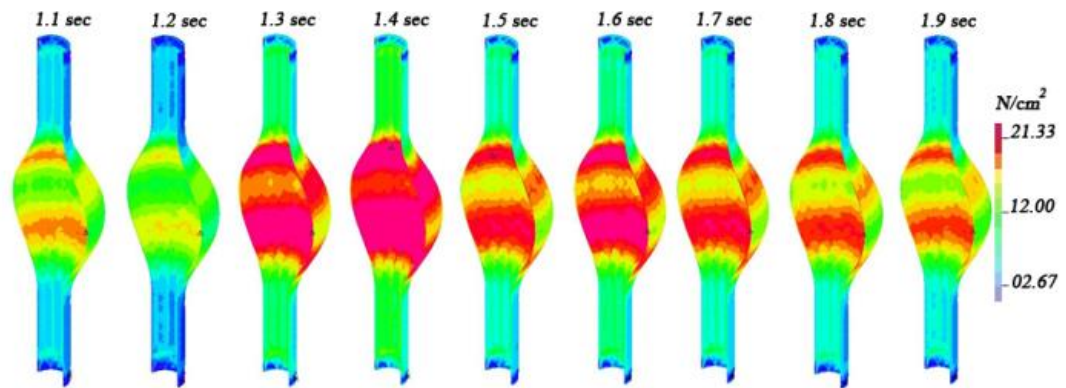

Figure. 3. The distributions of the Von Mises stress at different periods of the second cardiac cycle in model (D_{an}=6).

To show the effect of the maximum aneurysm diameter in Von Mises Stress in inner wall and outer wall. We have computed it along line on the inner wall and another one on the outer wall at peak systolic pressure condition and same thickness (0.15cm), and compared with different diameters as shown in Fig. 4. The Von Mises stress on the inner wall is higher than the outer wall. And the different between maximum Von Mises stress on the outer wall and inner wall decreased as the diameter increase. For example at Dan=3 cm, the Von Mises Stress on the inner wall is 11% higher than the outer wall and the different reduce as the diameter increase, where at Dan=10cm is 3%. The Von Mises stress on the inner and outer wall increase as the diameter increase, where at the small diameter (3cm, and 4cm) the maximum Von Mises stress occurs at the maximum diameter, which agree with Laplace equation[4]. But as the diameter increase to 5 cm the maximum Von Mises stress does not occur in the maximum diameter, but near to start and end of aneurysm, and the Von Mises stress in the midsection is around 8 % less than the maximum Von Mises stress. As the diameter increase, the location of maximum Von Mises stress move to the start and end of the aneurysm, and increase the different between the maximum Von Mises stress and the Von Mises stress in the midsection, where reach to 40% at 10 cm . However it should be noted that the Von Mises stress distribution is effected by the aneurysm diameter, and the

maximum Von Mises stress is not located at maximum diameter, but rather, where the local wall curvature is high. Which agree with the recent studies [34, 50, 51].

As evident by Fig. 3, and Fig. 4, the diameter of aneurysm have a significant effect on the magnitude and the distribution of the Von Mises Stress, and the wall curvature of the aneurysm has a strongly influences on the location of the Von Mises Stress. To fine the relationship between the Maximum Von Mises Stress and the maximum aneurysm diameter, the linear least squares method have been used as shown in Fig. 5. The linear correlation was observed (R^2= 0.9418), which agree with the finding by Doyle el. al[52], and Georgakaraka et al. [34].
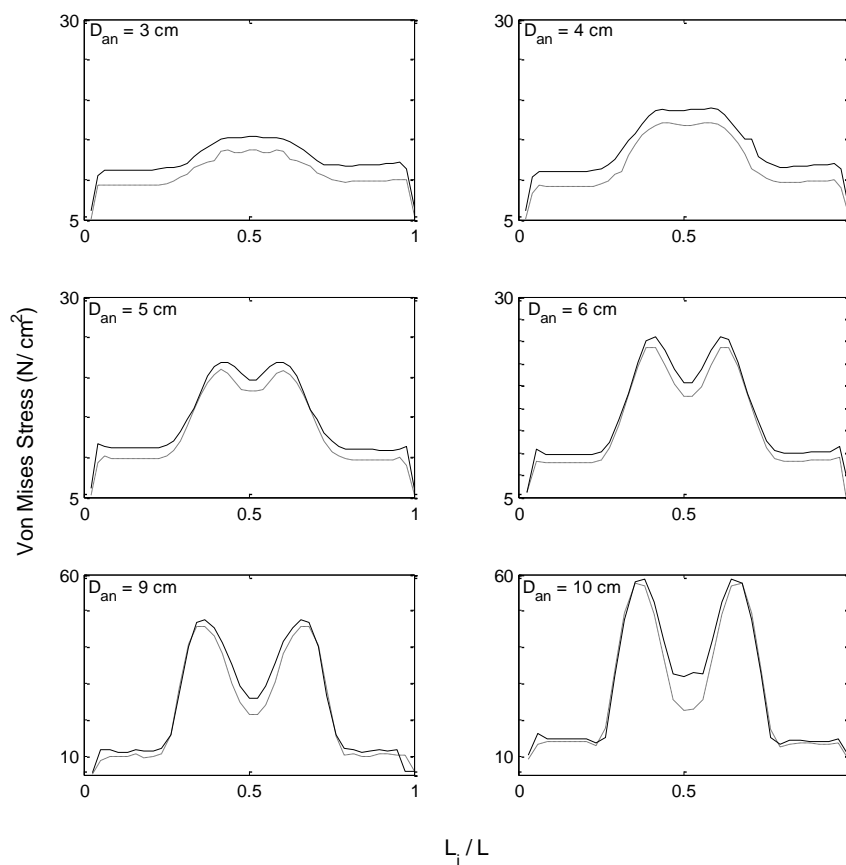

Figure. 4. The Von Mises Stress along the line on the inner wall (line),and the outer wall (dash line) with different diameter at peak systolic pressure condition.
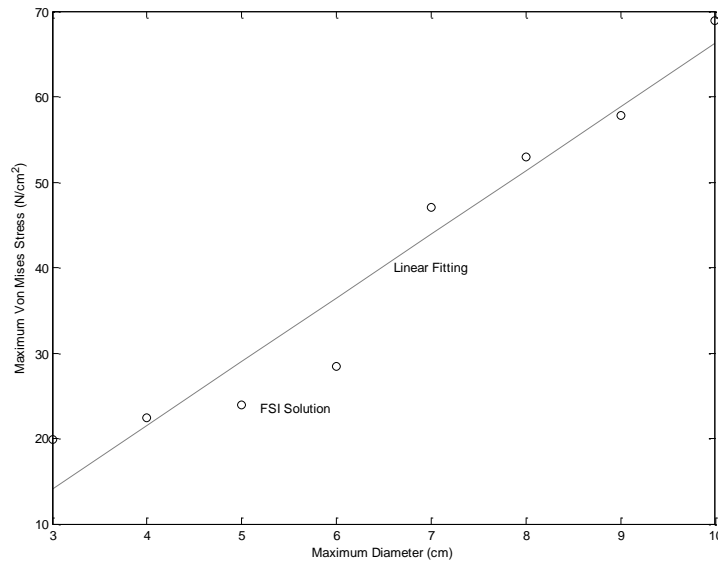
Figure. 5. The maximum Von Mises stress as a function of the maximum diameter of aneurysm

4. Conclusions

Fully coupled FSI simulations have employed to study the effect of the aneurysm diameter, on the velocity, and wall stress distribution. The aneurysm diameter effects the flow pattern by increase the size of vortices and also effect the direction of flow. The maximum wall stress occurs in the inner wall and the difference between the inner and outer wall decreased as the diameter increase. The maximum Von Mises stress increase linear as the maximum diameter increase ($R^2 = 0.9418$), and move to the ends of aneurysm, where the large wall curvature. However, this study suggests that the aneurysm diameter, as an important parameter to predict the risk of rupture. Of AAA aneurysm.

References

[1] M. law, Screening for abdominal aortic aneurysms, British Medical Bulletin, 54 (1998) 903-913.

[2] F.A. Lederle, R.L. Kane, R. MacDonald, Timothy J. Wilt, Systematic Review: Repair of Unruptured Abdominal Aortic Aneurysm, Annals of Internal Medicine, 146 (2007) 735-741.

[3] R. Gillum, Epidemiology of aortic aneurysm in the United States, Journal of Clinical Epidemiology, 48 (1995) 1289-1298.

[4] D.A. Vorp, Biomechanics of Abdominal Aortic Aneurysm, Journal of Biomechanics, 40 (2007) 1887-1902.

[5] T.M. McGloughlin, B.J. Doyle, New Approaches to Abdominal Aortic Aneurysm Rupture Risk Assessment : Engineering Insights With Clinical Gain, Journal of the American Heart Association, 30 (2010) 1687-1694.

[6] A. Abbas, R. Attia, A. Smith, M. Waltham, Can We Predict Abdominal Aortic Aneurysm (AAA) Progression and Rupture by Non-Invasive Imaging?—A Systematic Review, International Journal of Clinical Medicine, 2 (2011) 484-499.

[7] E. Choke, G. Cockerill, W.R.W. Wilson, S. Sayed, J. Dawson, I. Loftus, M.M. Thompson, A Review of Biological Factors Implicated in Abdominal Aortic Aneurysm Rupture, European Journal of Vascular and Endovascular Surgery, 30 (2005) 227-244.

[8] R. Limet, N. Sakalihassan, A. Albert, Determination of the Expansion Rate and Incidence of Rupture of Abdominal Aortic Aneurysms, Journal of Vascular Surgery 14 (1991) 540-548.

[9] J. Powell, L. Brown, J. Forbes, F. Fowkes, R. Greenhalgh, C. Ruckley, S. Thompson, Final 12-Year Follow-up of Surgery Versus Surveillance in the UK Small Aneurysm Trial, British Journal of Surgery, 94 (2007) 702-708.

[10] F.A. Lederle, G.R. Johnson, S.E. Wilson, D.J. Ballard, W.D. Jordan, J. Blebea, F.N. Littooy, J.A. Freischlag, D. Bandyk, J.H. Rapp, A.A. Salam, Rupture Rate of Large Abdominal Aortic Aneurysms in Patients Refusing or Unfit for Elective Repair Joutnal American Medical Association, 287 (2002) 2968-2972.

[11] T. Hatakeyama, H. Shigematsu, T. Muto, Risk Factors for Rupture of Abdominal Aortic Aneurysm Based on Three-Dimensional Study, Journal of Vascular Surgery, 33 (2001) 453-461.

[12] S. Kyriacou, J. Humphrey, Influence of Size, Shape and Properties on the Mechanics of Axisymmetric Saccular Aneurysms, Journal of Biomechanics, 29 (1996) 1015-1022.

[13] M. L.Raghavan, B. Ma, R.E. Harbaogh, Quantified Aneurysm Shape and Rupture Risk, Journal of Neurosurgery, 102 (2005) 355–362.

[14] D.A. Vorp, M.L. Raghavan, M.W. Webster, Mechanical Wall Stress in Abdominal Aortic Aneurysm: Influence of Diameter and Asymmetry, Journal of Vascular Surgery, 27 (1998) 632-639.

[15] A.J. Hall, E.F.G. Busse, D.J. McCarville, J.J. Burgess, Aortic Wall Tension as a Predictive Factor for Abdominal Aortic Aneurysm Rupture: Improving the Selection of Patients for Abdominal Aortic Aneurysm Repair, Annals of Vascular Surgery, 14 (2000) 152-157.

[16] J.V. Geest, E.S.D. Martino, A. Bohra, M.S. Makaroun, D.A. Vorp, A Biomechanics-Based Rupture Potential Index for Abdominal Aortic Aneurysm Risk Assessment Demonstrative Application, New York Academy of Sciences, 1085 (2006) 11–21.

[17] L. Speelman, A. Bohra, E.M.H. Bosboom, G.W.H. Schurink, F.N.v.d. Vosse, M.S. Makaroun, D.A. Vorp, Effects of Wall Calcifications in Patient-Specific Wall Stress Analyses of Abdominal Aortic Aneurysms, Journal of Biomechanical Engineering, 129 (2007) 105-109.

[18] D.A. Vorp, J.P.V. Geest, Biomechanical Determinants of Abdominal Aortic Aneurysm Rupture, Journal of the American Heart Association, 25 (2005) 1558-1566.

[19] M. Fillinger, M. Raghavan, S. Marra, J. Cronenwett, F. Kennedy, In Vivo Analysis of Mechanical Wall Stress and Abdominal Aortic Aneurysm Rupture Risk, Journal of Vascular Surgery 36 (2002) 589-597.

[20] M.L. Raghavan, M.F. Fillinger, S.P. Marra, B.P. Naegelein, F.E. Kennedy, Automated Methodology for Determination of Stress Distribution in Human Abdominal Aortic Aneurysm, Jornal of Biomechanical Engineering, 127 (2005) 868-871.

[21] B.J. Doyle, A. Callanan, M.T. Walsh, P.A. Grace, T.M. McGloughlin, A Finite Element Analysis Rupture Index (FEARI) as an Additional Tool for Abdominal Aortic Aneurysm Rupture Prediction, Vascular Disease Prevention, 6 (2009) 114-121.

[22] M. Fillinger, S. Marra, M. Raghavan, F. Kennedy, Prediction of Rupture Risk in Abdominal Aortic Aneurysm During Observation: Wall Stress Versus Diameter, Journal of Vascular Surgery 37 (2003) 724-732.

[23] M.L. Raghavan, D.A. Vorp, M.P. Federle, M.S. Makaroun, M.W. Webster, Wall Stress Distribution on Three Dimensionally Reconstructed Models of Human Abdominal Aortic Aneurysm, Journal of Vascular Surgery 31 (2000) 760-769.

[24] M. Truijers, J.A. Pol, L.J. SchultzeKool, S.M. van Sterkenburg, M.F. Fillinger, J.D. Blankensteijn, Wall Stress Analysis in Small Asymptomatic, Symptomatic and Ruptured Abdominal Aortic Aneurysms, European Journal of Vascular and Endovascular Surgery, 33 (2007) 401-407.

[25] Z.-Y. Li, U. Sadat, J. U-King-Im, T.Y. Tang, D.J. Bowden, P.D. Hayes, J.H. Gillard, Association Between Aneurysm Shoulder Stress and Abdominal Aortic Aneurysm Expansion : A Longitudinal Follow-Up Study, Journal of The American Heart Association, 122 (2010) 1815-1822.

[26] A.K. Venkatasubramaniam, M.J. Fagan, T. Mehta, K.J. Mylankal, B. Ray, G. Kuhan, I.C. Chetter, P.T. McCollum, A Comparative Study of Aortic Wall Stress Using Finite Element Analysis for Ruptured and Non-ruptured Abdominal Aortic Aneurysms, Eur J Vasc Endovasc Surg, 28 (2004) 168-176.

[27] C.M. Scotti, E.A. Finol, Compliant Biomechanics of Abdominal Aortic Aneurysms: a Fluid-Structure Interaction Study, Computers & Structures, 85 (2007) 1097-1113.

[28] K.M. Khanafer, J.L. Bull, R. Berguer, Fluid-Structure Interaction of Turbulent Pulsatile Flow within a Flexible Wall Axisymmetric Aortic Aneurysm Model, European Journal of Mechanics - B/Fluids, 28 (2009) 88-102.

[29] K.H. Fraser, M.-X. Li, W.T. Lee, W.J. Easson, P.R. Hoskins, Fluid–Structure Interaction in Axially Symmetric Models of Abdominal Aortic Aneurysms, Part H: Journal of Engineering in Medicine, 223 (2008) 195-209.

[30] J.H. Leung, A.R. Wright, N. Cheshire, J. Crane, S.A. Thom, A.D. Hughes, Y. Xu, Fluid Structure Interaction of Patient Specific Abdominal Aortic Aneurysms: a Comparison with Solid Stress Models

BioMedical Engineering OnLine, 5 (2006) 1-15.

[31] J.F. Rodríguez, C. Ruiz, M. Doblaré, G.A. Holzapfel, Mechanical Stresses in Abdominal Aortic Aneurysms: Influence of Diameter, Asymmetry, and Material Anisotropy, Journal of Biomechanical Engineering, 130 (2008) 1-10.

[32] D. Elger, D. Blackketter, R. Budwig, K.J. KH., The Influence of Shape on the Stresses in Model Abdominal Aortic Aneurysms., Journal of Biomechanical Engineering, 118 (1996) 326-332.

[33] F. Helderman, I.J. Manoch, M. Breeuwer, U. Kose, O. Schouten, M.R.M.v. Sambeek, D. Poldermans, P.T.M. Pattynama, W. Wisselink, A.F.W.v.d. Steen, R. Krams, A Numerical Model to Predict Abdominal Aortic Aneurysm Expansion Based on Local Wall Stress and Stiffness, Medical & Biological Engineering & Computing, 46 (2008) 1121-1127.

[34] E. Georgakarakos, C.V. Ioannou, Y. Kamarianakis, Y. Papaharilaou, T. Kostas, E. Manousaki, A.N. Katsamouris, The Role of Geometric Parameters in the Prediction of Abdominal Aortic Aneurysm Wall Stress, European Journal of Vascular and Endovascular Surgery, 39 (2010) 42-48.

[35] C.B. Washington, J. Shum, S.C. Muluk, E.A. Finol, The Association of Wall Mechanics and Morphology: A Case Study of Abdominal Aortic Aneurysm Growth, Journal of Biomechanical Engineering, 133 (2011) 1-6.

[36] S. I.Bernad, E. S.Bernad, T. Barbat, R. Susan-Resiga, V. Albulescu, Effects of Asymmetry in Patient-Specific Wall Shear Stess Analyses of Abdominal Aortic Aneurysm, Journal of Chinese Clinical Medicine, 4 (2009) 1-14.

[37] C.M. Scotti, A.D. Shkolnik, S.C. Muluk, E.A. Finol, Fluid-Structure Interaction in Abdominal Aortic Aneurysms: Effects of Asymmetry and Wall Thickness, BioMedical Engineering OnLine, 4 (2005) 1-22.

[38] Z. Li, C. Kleinstreuer, A Comparison Between Different Asymmetric Abdominal Aortic Aneurysm Morphologies Employing Computational Fluid-Structure Interaction Analysis, European Journal of Mechanics - B/Fluids, 26 (2007) 615-631.

[39] E.A. Finol, K. Keyhani, C.H. Amon, The Effect of Asymmetry in Abdominal Aortic Aneurysms Under Physiologically Realistic Pulsatile Flow Conditions, Journal of Biomechanical Engineering 125 (2003) 207-217.

[40] C.M. Scotti, J. Jimenez, S.C. Muluk, E.A. Finol, Wall Stress and Flow Dynamics in Abdominal Aortic Aneurysms: Finite Element Analysis vs. Fluid–Structure Interaction, Computer Methods in Biomechanics and Biomedical Engineering, 11 (2008) 301-322.

[41] H. Kohno, K.-J.u. Bathe, A Flow-Condition-Based Interpolation Finite Element Procedure for Triangular Grids, International Journal for Numerical Methods in Fluids, 51 (2006) 673-699.

[42] Z. Li, C. Kleinstreuer, Analysis of Biomechanical Factors Affecting Stent-Graft Migration in an Abdominal Aortic Aneurysm Model, Journal of Biomechanics, 39 (2006) 2264-2273.

[43] E.A. Finol, C.H. Amon, Flow-Induced Wall Shear Stress in Abdominal Aortic Aneurysms: Part II – Pulsatile Flow Hemodynamics, Computer Methods in Biomechanics and Biomedical Engineering, 5 (2001) 319–328.

[44] T.W. Taylor, T. Yamaguchi, Three-Dimensional Simulation of Blood Flow in an Abdominal Aortic Aneurysm—Steady and Unsteady Flow Cases, Journal of Biomechanical Engineering, 116 (1994) 88-97.

[45] R. Adolph, D. Vorp, D.S. DL, M. Webster, M. Kameneva, S. Watkins, Cellular Content and Permeability of Intraluminal Thrombus in Abdominal Aortic Aneurysm, Journal of Vascular Surgery, 25 (1997) 916-926.

[46] C. Taylor, T. Hughes, C. Zarins, Finite Element Modeling of Three-Dimensional Pulsatile Flow in the Abdominal Aorta: Relevance to Atherosclerosis, Annals of Biomedical Engineering, 26 (1998) 975-987.

[47] M. Bonert, R.L. Leask, J. Butany, C.R. Ethier, J.G. Myers, K.W. Johnston, M. Ojha, The Relationship Between Wall Shear Stress Distributions and Intimal Thickening in the Human Abdominal Aorta, BioMedical Engineering OnLine, 2 (2003) 1-14.

[48] A. Borghia, N.B. Wooda, R.H. Mohiaddinb, X.Y. Xua, Fluid–Solid Interaction Simulation of Flow and Stress Pattern in ThoracoAbdominal Aneurysms: A Patient-Specific Study, Journal of Fluids and Structures, 24 (2008) 270-280.

[49] Y. Papaharilaou, J.A. Ekaterinaris, E. Manousaki, A.N. Katsamouris, A Decoupled Fluid Structure Approach for Estimating Wall Stress in Abdominal Aortic Aneurysms, Journal of Biomechanics, 40 (2007) 367-377.

[50] M.S. Sacks, D.A. Vorp, M.L. Raghavan, M.P. Federle, M.W. Webster, In Vivo Three-Dimensional Surface Geometry of Abdominal Aortic Aneurysms, Annals of Biomedical Engineering,, 27 (1999) 469-479.

[51] G. Giannoglou, G. Giannakoulas, J. Soulis, Y. Chatzizisis, T. Perdikides, N. Melas, G. Parcharidis, G. Louridas, Predicting the Risk of Rupture of Abdominal Aortic Aneurysms by Utilizing Various Geometrical Parameters: Revisiting the Diameter Criterion, Angiology, 57 (2006) 487-494.

[52] B.J. Doyle, A. Callanan, P.E. Burke, P.A. Grace, M.T. Walsh, D.A. Vorp, T.M. McGloughlin, Vessel Asymmetry as an Additional Diagnostic Tool in the Assessment of Abdominal Aortic Aneurysms, Journal of Vascular Surgery, 49 (2009) 446-454.

[53] Y. S.C.M, Steady and Pulsatile Flow Studies in Abdominal Aortic Aneurysm Models Using Particle Image Velocimetry, International Journal of Heat and Fluid Flow, 21 (2000) 74-83.

[54] A. M. Muftah "3D Fluid in an Elbow Meter-CFD Model" SUSJ Journal, Sirte University, Vol. 4, Issue 1, June 2014

[55] A. Muftah "CFD Modeling of Elbow and Orifice Meters" SUSJ Journal, Sirte University, Vol. 7, Issue 1, June 2017, pp 15-32